



Multiscale Analysis of the Polymeric Insulators Degradation in Simulated Arid Environment Conditions: Cross-Correlation Assessment

Y. A. Bencherif^{1,2} · A. Mekhaldi¹ · J. Lobry² · M. Olivier³ · M. Poorteman³ · L. Bonnaud⁴

Received: 2 February 2019 / Revised: 2 May 2019 / Accepted: 3 June 2019
© The Korean Institute of Electrical Engineers 2019

Abstract

The aim of this study is to highlight the joint evolution of the chemical, morphological, thermal and dielectric behaviors upon the UV weathering of an industrial ethylene-propylene-diene monomer (EPDM) rubber. This latter is used as a housing of composite high voltage insulators which are installed in the Algerian desert. This material was submitted to photochemical aging by irradiating UVA rays ($\lambda = 340$ nm) at a temperature of 45 °C in order to simulate the witnessed site conditions. It was shown that the degradation process leading to the formation of oxygenated species and the depolymerization of the material are responsible of the coupling which may appear between the realized measurements. Using Kendall rank correlation analysis, joint evolution models were established. Those models introduce a novel assessment approach of the chemical and morphological status of the aged rubber using electrical and dielectric measurements.

Keywords EPDM · Insulator · UV Aging · Cross-correlation · Characterization

1 Introduction

Polymers such as ethylene-propylene-diene monomer (EPDM), which is a type of synthetic rubber composed of ethylene, propylene and unsaturated diene [1, 2], are applied in various technical fields due to their advantages in term of ease of production, light weight, ductility, good mechanical resistance and better contamination behavior [3–5]. Among the fastest growing applications of the synthetic rubbers, we can spot the composite high voltage insulators with EPDM housing. Further to the outdoor use of the latter, the bulk properties of the insulation material are affected due to its

exposition to stress conditions (radiation, heat, ozone, etc.) [2, 6]. The polymer's instability to weathering is one of the major issues which concern the insulation materials industry. This instability is caused by several reactions including rearrangements of the chemical structure, formation of oxidation, cross-linking and chain scission [7]. Thus, the comprehension of the mechanisms leading to these reactions by the study of the material's behavior against each type of stress condition is critical for the assessment of the material's life time [2].

Among the disadvantages of the natural aging of studied samples, we can notice the complex reproducibility, time consuming procedures and the difficulty to segregate the stress conditions [2, 8, 9]. In this regard, in order to study the separate effect of each type of stress on the material within a reasonable term, a laboratory artificial aging is required. Several works have been done to study the impact of the aging on the characteristics of the materials and the processes responsible of their degradation. Most of these works focused on a limited number of aspects of aging leading to a partial view of the material's degradation. Zhao et al. [6, 8, 10] carried out a weathering of EPDM to study its impact on morphological, thermal and chemical properties of the material. Ehsani et al. [11] studied the impact of the heat aging on the electric properties of the EPDM. Other studies

✉ Y. A. Bencherif
yacine.bencherif@gmail.com

¹ Laboratoire de Recherche en Electrotechnique, Ecole Nationale Polytechnique, Rue des Frères Oudak, Hassen Badi, B.P. 182, El-Harrach, 16200 Algiers, Algeria

² Department of General Physics, University of Mons, 9, Rue Houdain, B7000 Mons, Belgium

³ Institute of Research in Science and Engineering of Materials, University of Mons, 56, Rue de l'Épargne, 7000 Mons, Belgium

⁴ Materia Nova asbl, Parc Initialis, Avenue Copernic 1, 7000 Mons, Belgium

[5, 12] focused on the impact of a service aging on the thermal, chemical and dielectric properties of the housing of a composite high voltage insulator.

However, to our knowledge, no works treated the long-term photochemical aging of EPDM used as a housing of a composite insulator by carrying a multiscale analysis studying the impact of the aging on the thermal, chemical, morphological, mechanical, electric and dielectric properties. The compilation of the latter allows us to highlight the coupling which may exist between electric, dielectric and physico-chemical properties of the material.

The aim of this study is to investigate the aging behavior of the EPDM insulators used in the Algerian desert. The studied samples were subjected to an artificial aging under UV weathering in order to simulate the real site conditions. Several techniques were used with the purpose to track the effect of the aging on the different structural scales of the material. As detailed in Sects. 2 and 3, we tried to highlight the processes occurring in the material with the purpose to seek the joint evolution of the electric and dielectric properties of the material against its morphological, chemical, thermal and mechanical behaviors. In this regard, a cross-validation analysis was established using the Kendall rank correlation technique leading to the elaboration of joint evolution models. The latter introduces a useful support for the elaboration of an assessment monitoring guideline of high voltage composite insulators. Studies which applied similar aging conditions [13, 14] didn't consider the cross-correlation aspect in the evolution of the material's properties due to the application of a limited number of characterization techniques.

2 Materials and Methods

2.1 Materials

The EPDM used within our study was provided by Sediver, France. It is composed of aluminum tri-hydrate (ATH) as filler, plasticizers, a peroxide, and an agent for stabilization complying with the composition given in Table 1. The studied samples have been conditioned in sheets of 2 mm thickness with various dimensions adapted to the dedicated characterization techniques.

2.2 Material Aging

Photochemical aging was applied on EPDM sheets directly irradiated by UVA rays ($\lambda = 340$ nm) at a temperature of 45 °C. The irradiance of the lamps was 0.89 W/m²/nm which simulates the direct solar UV radiation exposure as recommended by the standard ASTM G154 [12]. No condensation was applied in order to simulate the dry conditions existing

Table 1 Composition of studied EPDM

Composition	Quantity (parts)
EPDM (ethylidene norbornene)	100
Alumina trihydrate (ATH)	240
Plasticisers	40
Anti-oxidants	5
Dicumyl peroxide	6

in the Algerian desert. The chosen temperature is related to the peak values recorded along the year. The samples were submitted to different aging time intervals up to 2160 h. As indicated in the literature, 200 h of artificial weathering are equivalent to 1 year of actual outdoor UV exposure [15–17].

2.3 Thermal Characterization

Thermal analysis involves the measurement of material's properties as a function of temperature. Despite the fact that thermal analysis covers a wide range of techniques, differential scanning calorimetry (DSC), thermogravimetric analysis (TGA) and dynamic mechanical analysis (DMA) are the techniques we were able to use within our study.

DSC analysis was carried out using Q2000 device from TA instrument under constant nitrogen gas flow. Thermograms for samples of approximately 10 mg were recorded in one run. The heating was from – 90 to 140 °C, followed by cooling from 140 to – 100 °C, at a rate of 5°C/min. The degree of crystallinity of samples was calculated by considering 270 J/g as melting enthalpy value of the EPDM when it crystallizes completely [18].

Thermogravimetric analysis (TGA) was conducted by monitoring the weight-loss of the studied EPDM samples in order to evaluate their thermal stability. This analysis was performed with a TGA Q50 device from TA Instruments. Within our study, samples of approximately 10 mg were analyzed by a heating at a constant rate of 10 °C/min between 25 and 800 °C. All TGA experiments were performed under constant flow of nitrogen in order to remove all corrosive gases formed during degradation and to avoid further thermo-oxidative degradation.

DMA is a measure of the deformation of a material in response to vibration forces [11]. Unlike the tensile test, the DMA measurements are influenced preferentially by the properties of the surface layers of the tested samples [19]. DMA of the EPDM samples was performed in dual cantilever mode using a TA instruments Q800 apparatus. The samples (35 mm × 12 mm × 2.3 mm) were tested under constant deformation amplitude of 10 µm at a frequency of 1 Hz and under a temperature ramp of 3 °C/min over the temperature range of – 100 to 140 °C. The mechanical loss

factor ($\tan \delta$) was measured as a function of temperature for all the samples under identical conditions.

2.4 Chemical Characterization

Chemical analysis of the aged samples was carried including the Infrared spectroscopy technique (FTIR) and the Energy dispersive X-ray (EDX) analysis.

The FTIR technique is useful in identifying organic and inorganic compounds by comparing frequencies and intensities with reference spectra [20]. This technique is recommended for thick samples similar to those analyzed in this paper. Chemical changes upon aging were performed with an ATR-FTIR spectrometer (Attenuated Total reflectance—Bruker IFS66v/s). 32 scans were used for each sample working with a resolution of 4/cm in a spectra range of 4000–400/cm. In order to make a deep understanding on the changes which may occur in the material during the aging, EDX analysis was performed to obtain the element composition of the studied samples. The EDX analysis was carried out with a SEM and its adjunct EDX analyzer (SEM Hitachi SU-8020, Japan) under an accelerating voltage of 10 kV leading to an estimated depth of 1 μm for the analyzed layer.

2.5 Surface Morphology Characterization

The characterization of the morphology of the surface of the studied samples was done using the visualization of the surface with scanning electron microscope (SEM), measure of the contact angle, and colorimetry measurement.

The surface morphology of aged EPDM samples were investigated by scanning electron microscope (SEM) using an SU-8020 scanning electron microscope (Hitachi, Japan) at an accelerating voltage of 5 kV.

A hydrophobic surface has a water repellent property, whereas a hydrophilic surface can be easily wetted. The contact angle that a drop makes when it comes into contact with a solids surface is a measure of the surface wettability. The hydrophobicity evaluation of housing insulation is commonly made according to STRI guide [21]. This method is commonly used at site. However, it has an intrinsic inaccuracy because of its subjective image analysis which depends on the operator's criteria [22]. In order to analyze the contact angle more accurately, the hydrophobicity of the housing polymer was evaluated using GDX digidrop goniometer with a video camera system and the Visiodrop software. It places a 3–5 μl drop of distilled water on the previously cleaned polymeric surface using a Teflon-coated needle. Then, a photograph of it is taken with a high resolution digital camera. By digital image analysis and the use of special software, the contact angle is measured. The data of the contact angle were obtained from the mean of three to

four measurements that were made to different drops placed on the surface.

The colorimetry of the studied samples was measured using a SpectroDens spectro-densitometer of TECHKON. Lightness (L^*) and chromacity coordinates (a^* and b^*) were measured. Changes in color are expressed by changes in L^* , a^* and b^* , and by changes in the distance between two points in the three dimensional coordinated system. The total color change (ΔE^*_{ab}) was calculated using the following equation:

$$\Delta E^*_{ab} = \left[(\Delta L^*)^2 + (\Delta a^*)^2 + (\Delta b^*)^2 \right]^{1/2}. \quad (1)$$

Three measurements were taken on different locations of each sample. Three samples were analyzed at each aging status. The average of those 9 measures (3 areas \times 3 samples) was used for data analysis. The effect of the aging on the color change was analyzed.

2.6 Mechanical Characterization

For the mechanical characterization of the material, the hardness of the samples was measured. In this regard shore A hardness was measured by means of a pocket hardness meter (type CEAST, Torino/Italy) according to ISO/R 868. Three samples were tested. Three measures for each sample at different areas location were performed in order to get a reliable result.

2.7 Dielectric and Electric Properties Characterization

The dielectric loss factor ($\tan \delta$) of the material was measured in function of aging time by using a Schering bridge (TETTEX A.G ZURICH type 2904) under AC voltage of 1 kV, 50 Hz. A test cell consisting of two circular plane electrodes of 20 cm^2 surface and a guard electrode was used to eliminate the surface conduction effect [23]. The same test cell was used for the evaluation of the surface resistivity of the studied samples. In this regard, the resistance between two electrodes mounted on the surface of the samples was measured as an image of the surface resistivity. The voltage across a shunt resistance was measured as an image of the current passing through the material as per IEC62631-3-2.

2.8 Statistical Calculation of Correlation Coefficients

Correlation coefficients were generated by performing Kendall rank correlation analysis for all parameters using average values calculated from all original determinations. Kendall's tau (r_k) coefficient was preferred among the other correlation coefficients existing in the literature due to a better robustness

and efficiency for small samples [24]. Parameter τ_k is a measure which works better in detecting a non-linear relationship between two variables [25]. It can take a value from -1 to 1 . The higher the absolute value of τ_k the stronger the association between the two variables. Positive values suggest that higher values of one variable are associated with higher values of the other variable; negative values suggest that higher values of one are associated with lower values of the other [26].

3 Results and Discussion

3.1 Thermal Characterization

As shown in Fig. 1 corresponding to the DSC thermograms of the studied samples, the round shape of the peaks indicates that the material is semicrystalline [27]. The obtained results show a step change related to a glass transition temperature (T_g) and an endothermic peak corresponding to the melting of the ethylene component occurring at the melting temperature (T_m) [28].

We have to note that the relatively low value of the enthalpy of fusion is due to the amorphous proportion of the EPDM. For UV aging, the DSC thermograms don't show a significant change of T_g along the aging time as indicated in Table 2. However, we can observe a slight decrease of the melt enthalpy ΔH_m along the aging time. This depression implies a reduction of the degree of crystallinity χ of the material which is calculated using the following equation:

$$\chi = \frac{\Delta H_m}{\Delta H_m^0} \times 100. \quad (2)$$

With ΔH_m^0 is the melt enthalpy of a completely crystalline sample.

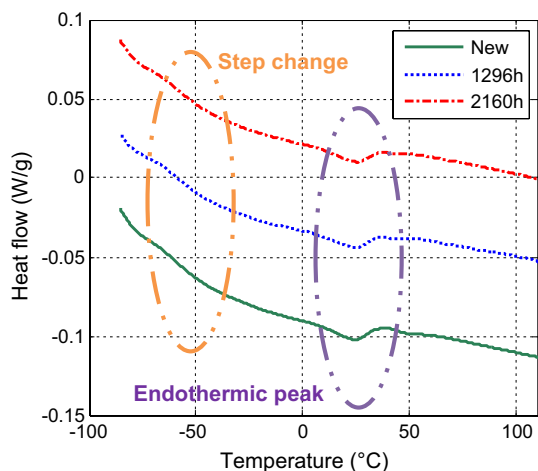


Fig. 1 DSC heating thermograms of new and UV aged samples

The reduction of the degree of crystallinity χ can be due to the scissions of chains which may be accompanied by crosslinking [29–31]. This bulk degradation of the EPDM disrupts the crystalline order of the polymer [27, 32].

TGA is a useful technique to assess the thermal stability of the studied material as well as the amount of the components present in the polymer. As can be observed from Fig. 2, weight percentage of ash residues for UV aged samples is almost the same as new samples, meaning that the loss of material's components is negligible for this type of aging.

The TGA and DTG results shown in Table 3 indicate that this type of degradation has no impact on the thermal stability of the material.

Due to the inherent sensitivity of DMA to the glass transition, this technique is ideal for identifying the T_g of highly filled systems [33]. More precisely, DMA allows measuring the thermomechanical transition associated to the glass transition of the material. Viscoelastic properties ($\tan \delta$ vs. temperature) of the studied material are illustrated in Fig. 3. The temperature corresponding to the maximum peak in the $\tan \delta$ vs. temperature plot was taken as the glass transition temperature. The cross-linkage of the material increases T_g , reduces $\tan \delta$ (max) and usually increases peak width [34].

We can notice from Fig. 3 that the aging time has induced the increase of the glass transition temperature. This phenomenon may be explained by a denser cross linkage and

Table 2 Parameters obtained from DSC measurement for UV aging

Sample	T_g (°C)	T_m (°C)	ΔH_m (J/g)	χ (%)
New	-61	26	1.31	0.48
1296 h aged	-60	26	1.05	0.38
2160 h aged	-60	27	1.00	0.37

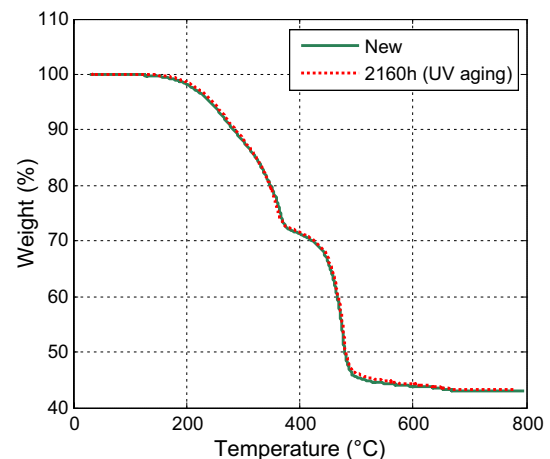
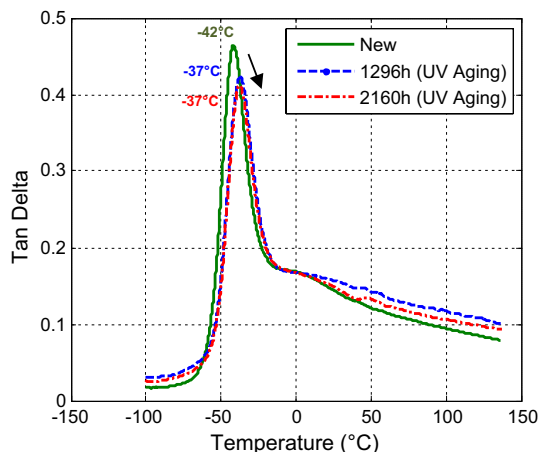


Fig. 2 TGA results of new and UV aged EPDM

Table 3 TGA & DTG results summary for UV aged EPDM

Sample	DTG peak temp. of 1st event (°C)	Onset temp. of 1st event (°C)	1st mass loss (%)	DTG peak temp. of 2nd event (°C)	Onset temp. of 2nd event (°C)	2nd mass loss (%)
New	365	128	28	475	392	27
1296 h aged	359	124	28	475	390	27
2160 h aged	354	134	28	477	392	28

**Fig. 3** Tan δ vs. temperature plots of industrial EPDM aged under UV rays (DMA Method)

reduction in free volume available for local segmental motions [35–38]. The increase of T_g can be also explained by a higher polarity and thus intermolecular attraction as a result of oxidative chain scission, and/or a higher relative filler content because of decomposition and volatilization of the polymer [39].

As pointed out in other studies [39], the observed behavior of the material through DMA analysis doesn't indicate whether only cross-linking reactions are occurring, or whether both chain scissions and cross-linking occur. The latter may slightly outweigh the effects of scissions.

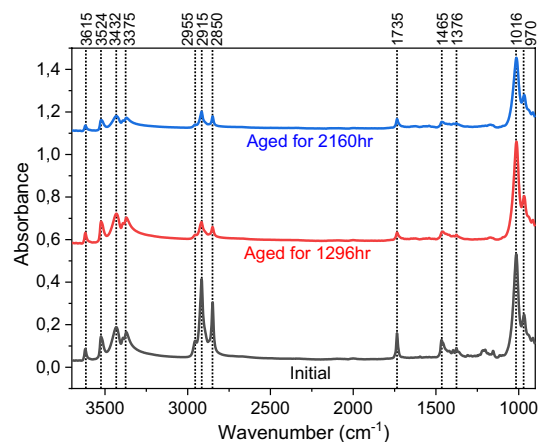
We can notice that the T_g value isn't the same when measured by DSC and DMA methods. Though it is agreed to assess the glass transition temperature through a single temperature, in reality it shows a transient behavior. DMA and DSC techniques measure different processes which lead to a difference in data. This difference can reach 25 °C as per the literature [40, 41].

3.2 Chemical Characterization

The ATR-FTIR technique is used in this study to identify the chemical reaction taking place during the aging of the material. In this regard the wavenumbers and their corresponding functional groups for the significant bands related to the studied material are shown in Table 4.

Table 4 Significant bands and functional groups of studied EPDM sample [4, 27, 42–45]

Wavenumber (/cm)	Absorption bond
3615, 3524, 3432, 3375	Al(OH) ₃
1465, 1376, 2915, 2955	CH ₃ (Methyl group)
2850	CH ₂ (Methylene group)
1259, 970	CH
1016, 791, 728, 665	Al–O
1750–1720	> C=O (Carbonyl group)
3370–3620	OH

**Fig. 4** ATR-FTIR spectra of EPDM after UV weathering

From Fig. 4 we can notice a loss of hydrocarbon groups in all aged samples. The observed peak at the area 1750–1720/cm can be assigned to ketone absorption. This peak, related to carbonyl group, is visible for the non-aged samples which means that the oxidation of the material started from its manufacturing [6]. However, we can observe from Fig. 5 that the carbonyl index (CI), which represents the relative intensities of the carbonyl band at 1735/cm relative to the methylene band at 2850/cm [46], increases with the aging time. It can be seen that the CI increased quickly at the first 1000 h of aging. In the following stage, the increase of CI becomes less important. The relationship between CI and the aging time regarding the applied conditions can be expressed as: $CI = 0.22634x(t + 30.04548)^{0.17286}$ with $R^2 = 0.96241$.

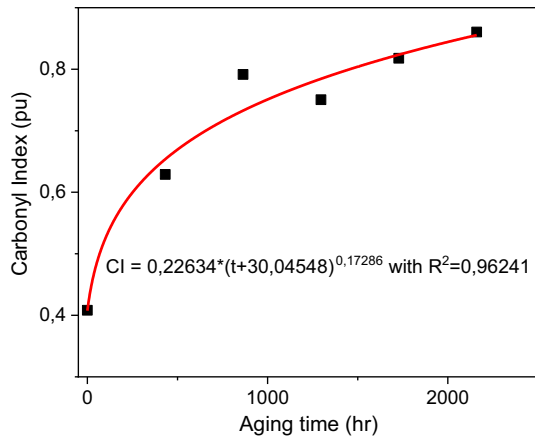


Fig. 5 Variation of the Carbonyl Index vs the aging time

Since oxygen appears in different organic functions in degradation products, such as alcohol, ketone and ester, it is difficult to link the degradation with a specific functional

group [10]. Table 5 shows the percentage of the weight composition and the atomic ratios O/C and Al/C for the analyzed samples. Those ratios were adopted in order to assess the degradation of the samples. From our measurements, we can observe that the ratios O/C and Al/C increase with the aging time. This result is complying with the FTIR analysis related to the oxidation and depolymerization processes which happened during the aging. Similar results were reported in other studies [10, 12, 47–49].

3.3 Surface Morphology Characterization

Figure 6 shows micrographs of EPDM samples before and after aging for different aging times. Apparently, the surface of the new EPDM sample was relatively smooth, compared with the other samples. With increasing aging time, small voids appeared. We can notice that the polymer outer layer of the sample is removed during aging. This layer is related to the surface finish of the molding process [22].

Table 5 Weight composition percentage of C, O and Al for EPDM aged thermally under UV rays

	C		O		Al		O/C	Al/C
	Weight (%)	Weight (%) error	Weight (%)	Weight (%) error	Weight (%)	Weight (%) error		
New	52.2	± 0.3	27.5	±0.4	18.9	± 0.1	0.52	0.36
432 h	28.7	± 0.3	46.2	±0.4	23.7	± 0.1	1.60	0.82
1296 h	19.5	± 0.3	47.3	±0.4	29.3	± 0.2	2.42	1.50
1728 h	19.8	± 0.3	51.3	±0.4	26.5	± 0.1	2.59	1.33
2160 h	17.2	± 0.3	49.9	±0.4	29.1	± 0.2	2.90	1.69

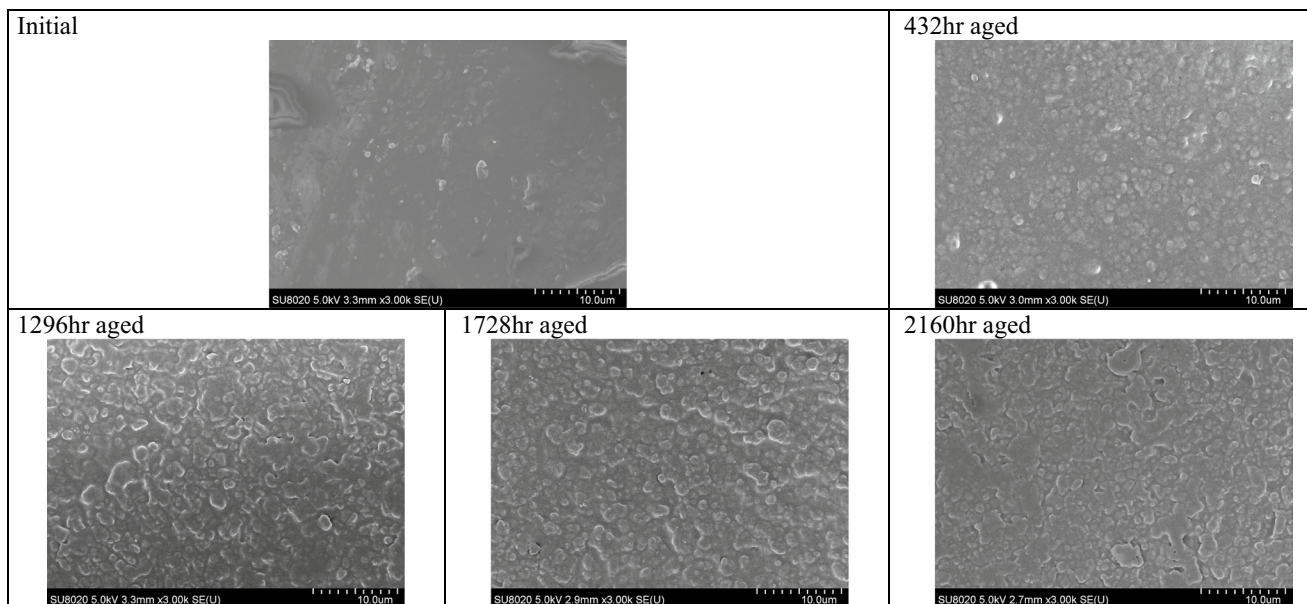


Fig. 6 Surface microstructure of photo-aged EPDM

From our observations with aging time, it can be noticed that the outer layer of the samples is eroded. Thus, the outer molded layer consisting mainly by polymer is substituted by a layer composed of polymer and fillers. This process has as a consequence to increase the roughness of the material. The hydrophobicity is, thus, a parameter which can be evaluated by SEM due to the possibility of that method to assess smoothness and contaminant extent [50].

From Fig. 7, we notice that the contact angle (CA) decreases monotonously and linearly with aging time. The decrease of the contact angle can be explained by the polymer's oxidation which generates polar groups such as carbonyl on the material's surface increasing the wettability [22].

The observed strong negative linear relationship between the contact angle and the exposure time can be expressed as: $CA = 108.66828 - 0.02109 * t$ with $R^2 = 0.9875$.

Figure 8 shows a clear color change during aging of the studied samples. We can observe the effect of the UV stress regarding the evolution of ΔE . We can observe a sharp increase at the beginning of the aging process and then stabilization.

3.4 Mechanical Characterization

From Fig. 9, it can be seen that the hardness of the material increases with the aging time. This observation coupled to the increase of the glass transition temperature, as shown in the thermal analysis of the samples, indicates the occurrence of a crosslinking. As per Tomer et al. the surface of the samples becomes harder because the polymer chains cannot adopt different configurations during stressing and are less flexible due to the crosslinkage of the material [4].

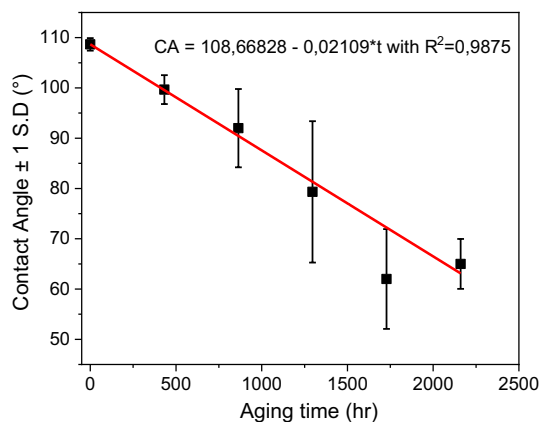


Fig. 7 Contact angle vs aging time for photo-aged samples

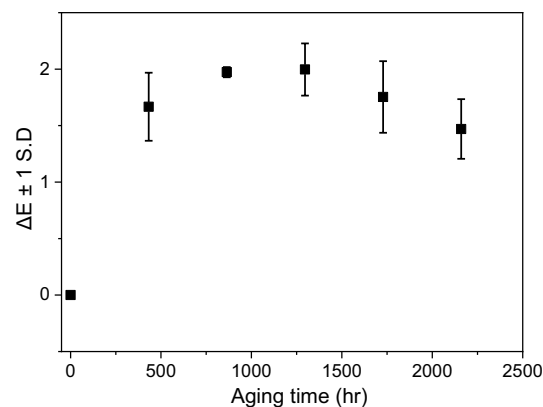


Fig. 8 Effect of photo-aging on total color change

3.5 Dielectric and Electric Properties Characterization

Measurements using our Schering Bridge have been carried out in order to get the surface resistances and the dielectric loss factor.

As seen during the thermal characterization, the loss factor measured with DMA technique is a significant parameter for the characterization of the equilibrium between the viscous and elastic state of the material in term of the antagonism between the chain scission and recombination including the cross-linking. The parallelism between the mechanical and dielectric behavior of the material was highlighted in previous studies [51] implying the involvement of the same mechanisms for the interpretation of the results [37, 52].

As indicated in Fig. 10, we observe a reduction of the loss factor with stabilization at a value of 0,015 after 1000 h of aging. The relationship between $\tan \delta$ and the aging time regarding the applied conditions can be expressed as: $\tan \delta = 0.03793 * (t + 59.05459) - 0.12467$ with $R^2 = 0.86705$.

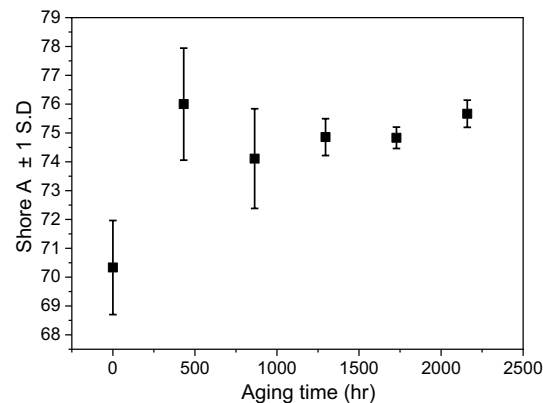


Fig. 9 Variation of the hardness vs the aging time

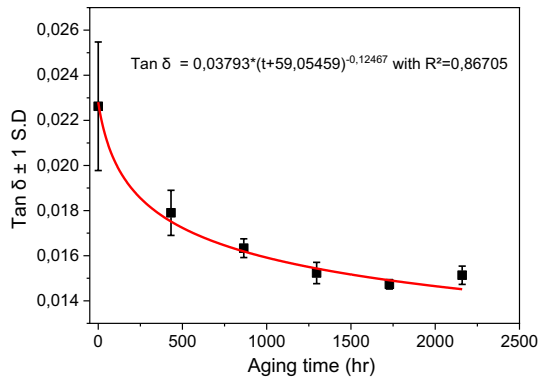


Fig. 10 Variation of the dielectric loss factor vs the aging time

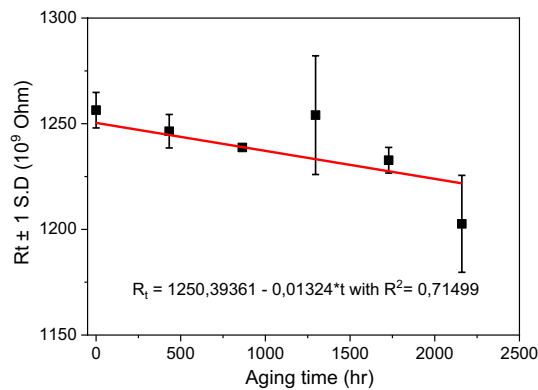


Fig. 11 Variation of the surface resistance vs the aging time

As indicated in Fig. 11, we can observe a reduction of the surface resistance of the material (R_t) along the aging. The decrease of surface resistance of the sample can be explained by the depolymerization of the material caused by the photo degradation. The relationship between R_t and the aging time regarding the applied conditions can be expressed as: $R_t = 1250.39361 - 0.01324 * t$ with $R^2 = 0.71499$.

3.6 Cross Correlation Assessment

The calculated results of Kendall rank correlation coefficient for each set of measurements is shown in the Table 6. The significance test results (p value matrix) are shown in Table 7. Within our study, we considered two sets of parameters to be correlated when the correlation coefficient is higher than 0.7 and p -value less than 5%.

From the obtained calculations, it appears that three pairs of parameters [(CI, R_t), (CA, $\text{Tan } \delta$) and (O/C, CI)] are strongly correlated along the UV aging. Two other pairs [(CI, $\text{Tan } \delta$) and (CA, CI)] are correlated but requires a larger set of samples in order to decrease the relatively high p -value.

Based on the above tables, joint evolution curves was plotted as indicated in Figs. 12, 13, 14, 15 and 16. It appears from each figures that a joint evolution model can be generated leading to the prediction of a parameter using the value of its correlated measurement.

Figure 12 is clear evidence that the realized measurements are in agreement with the degradation process

Table 6 Kendall rank correlation coefficient matrix

R_t	FTIR (CI)	CA	Color Change	Shore A	EDX (O/C)	EDX (Al/C)	
0.59	- 0.73	0.99	- 0.33	- 0.19	- 0.8	- 0.6	Tan δ
	- 0.86	0.59	0.06	- 0.33	- 0.8	- 0.6	R_t
		- 0.73	0.06	0.19	1	0.8	FTIR (CI)
			- 0.33	- 0.19	- 0.8	- 0.6	CA
				0.06	0.2	0.4	Color change
					0.2	0.4	Shore A
						0.8	EDX (O/C)

Table 7 p -value matrix

R_t	FTIR (CI)	CA	Color Change	Shore A	EDX (O/C)	EDX (Al/C)	
0.132	0.060	0.008	0.452	0.707	0.086	0.220	Tan δ
	0.024	0.132	1	0.452	0.086	0.220	R_t
		0.060	1	0.707	0.027	0.086	FTIR (CI)
			0.452	0.707	0.086	0.220	CA
				1	0.806	0.462	Color change
					0.806	0.462	Shore A
						0.086	EDX (O/C)

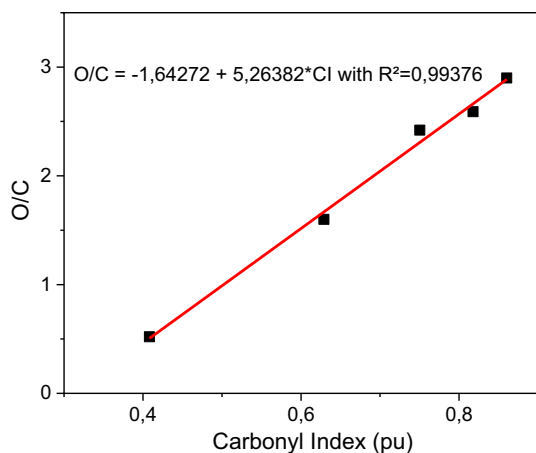


Fig. 12 Joint evolution of the O/C weight factor vs the Carbonyl Index along the UV aging

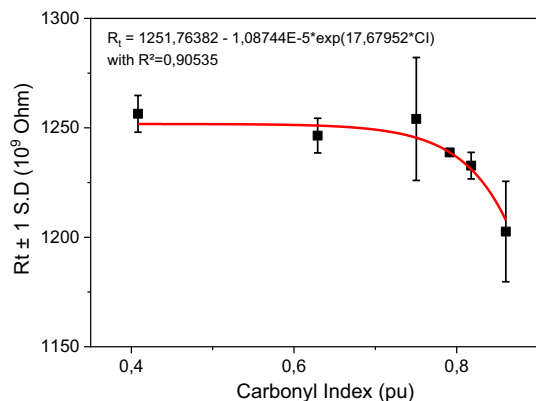


Fig. 13 Joint evolution of the tangential resistance vs the Carbonyl Index along the UV aging

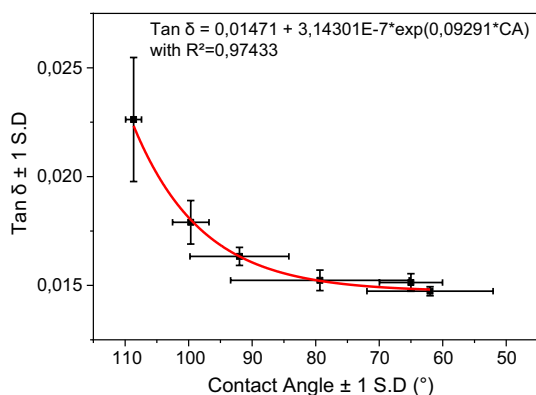


Fig. 14 Joint evolution of the dielectric loss factor vs the contact angle along the UV aging

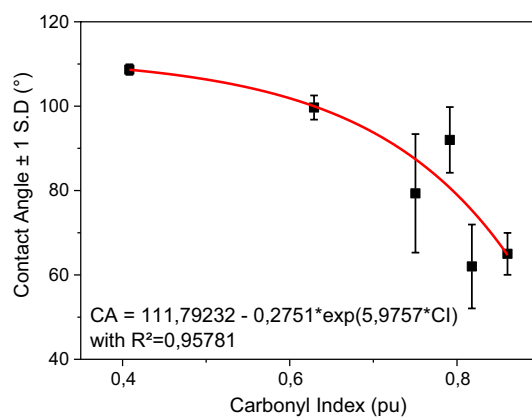


Fig. 15 Joint evolution of the contact angle vs the Carbonyl Index along the UV aging

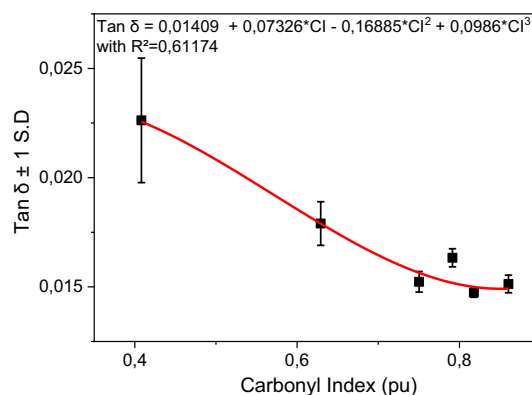


Fig. 16 Joint evolution of the dielectric loss factor vs the Carbonyl Index along the UV aging

which is supposed to appear along the UV aging. Indeed, the oxygen proportion is rising in a linear way with the carbonyl index. It is possible to state that each of these two measurements can substitute the other for the assessment of the oxidation level. The strong positive linear relationship between the O/C ratio and the Carbonyl Index can be expressed as: $O/C = -1.64272 + 5.26382 \cdot CI$ with $R^2 = 0.99376$.

From Fig. 13, we observe the strong correlation between the surface resistivity and the carbonyl index suggesting that the oxidation of the material has a direct impact on its surface conductivity. The relationship between R_t and the Carbonyl Index can be expressed as: $R_t = 1251.76382 - 1.08744E - 5 \cdot \exp(17.67952 \cdot CI)$ with $R^2 = 0.90535$.

As shown in Fig. 14, the strong correlation between the contact angle and the dielectric loss factor indicates that these parameters are governed by the same degradation processes. The relationship between $Tan \delta$ and the contact angle can be expressed as: $Tan \delta = 0.01471 + 3.14301E - 7 \cdot \exp(0.09291 \cdot CA)$ with $R^2 = 0.97433$.

As we can observe in Figs. 15 and 16, the oxidation of the material has a direct impact on the hydrophobicity and the dielectric loss factor. This degradation process leads to the establishment of relationships expressed as: $CA = 111.79232 - 0.2751 \cdot \exp(5.9757 \cdot CI)$ with $R^2 = 0.95781$ and $\tan \delta = 0.01409 + 0.07326 \cdot CI - 0.16885 \cdot CI^2 + 0.0986 \cdot CI^3$ with $R^2 = 0.61174$.

4 Conclusion

In this paper, we have carried out a multiscale analysis of EPDM based material used as a housing of a high voltage composite insulator. The latter was submitted to simulated arid environment aging. The joint evolution of the thermal, chemical, morphological, mechanical, electrical and dielectric behaviors was investigated. The results of this study led to the main conclusions listed as below:

- From the thermal analysis of the material, it appears that a crosslinking process takes place along the applied weathering.
- Upon weathering aging, it was not possible to detect any change of T_g by DSC method whereas modifications of the thermomechanical transition associated to the T_g of the material were observed by DMA analysis. DMA method is found to be more appropriate for the analysis of surface degraded samples than DSC technique.
- The TGA technique showed that the applied weathering didn't cause a degradation of the thermal stability of material's components.
- The formation of oxygenated species within the material continues along the aging. Their increase tends to be less important after 1000 h of aging.
- The atomic ratio O/C and the carbonyl index are correlated with linear trend along the applied UV weathering.
- The hydrophobicity of the EPDM is drastically affected by the UV aging. For the applied weathering, the surface contact angle decreases linearly along the aging time.
- The dielectric loss factor decreases along the applied weathering. Stabilization is observed after 1000 h of aging which is a similar behavior as measured for the carbonyl index.
- A depolymerization during the UV aging was witnessed in this study causing the decrease of the surface resistance.
- The established correlation between the surface resistivity and the carbonyl index indicates that the oxidation of the material has an impact on the surface conductivity only after a given threshold which is equal to 0.75. Antagonist behavior of the dielectric loss factor is observed. Indeed, $\tan \delta$ decreases drastically until the

carbonyl index reaches the threshold of 0.75 and then stabilizes.

- The surface contact angle decreases monotonously when the carbonyl index increases.
- The established regression models via the proved correlations are useful tools for experimental studies. Those models can be used for the prediction of the life time of the insulator's housing and a helpful support for the degradation assessment of the high voltage composite insulators.
- Our contribution consists in the establishment of the joint evolution models which make possible the assessment of the chemical and morphological status of the aged samples via electrical and dielectric measurements.
- Taking in consideration the established joint evolution models, the characterization campaigns of a set of samples can be optimized by reducing the measurements number.
- Further research can be done to study the cross-correlation which may occur for different type of stress condition as the marine environment or chemical pollution exposition.
- By enriching the obtained results with additional measurements to enlarge the characterization database, machine learning methods can be applied to create an artificial intelligence model used to predict the material's behavior along the aging time considering the chosen EPDM's based structure.

References

1. Bouguedad D, Mekhaldi A, Boubakeur A, Jbara O (2008) Thermal ageing effects on the properties of ethylene-propylene-diene monomer (EPDM). *Sciences des matériaux* 33:303–313
2. Bencherif YA, Mekhaldi A, Lobry J, Olivier M, Poorteman M (2018) Molecular macroscopic characterization of EPDM's aging used for outdoor high voltage insulators. In: 2018 international conference on electrical sciences and technologies in Maghreb (CISTEM), 2018, pp 1–5
3. Khattak A, Amin M (2016) Influence of stresses and fillers on the aging behaviour of polymeric insulators. *Rev Adv Mater Sci* 44:194–205
4. Tomer NS, Delor-Jestin F, Singh RP, Lacoste J (2007) Cross-linking assessment after accelerated ageing of ethylene propylene diene monomer rubber. *Polym Degrad Stab* 92:457–463
5. Sorichetti P, Matteo C, Lambri O, Manguzzi G, Salvatierra L, Herrero O (2007) Structural changes in EPDM subjected to ageing in high voltage transmission lines. In: *IEEE transactions on dielectrics and electrical insulation*, vol. 14, 2007
6. Zhao Q, Li X, Gao J (2009) Aging behavior and mechanism of ethylene-propylene-diene monomer (EPDM) rubber in fluorescent UV/condensation weathering environment. *Polym Degrad Stab* 94:339–343
7. Rivaton A, Gardette JL, Mailhot B, Morlat Therlas S (2005) Basic aspects of polymer degradation. In: *Macromolecular Symposia*, 2005, pp 129–146

8. Zhao Q, Li X, Gao J (2007) Aging of ethylene–propylene–diene monomer (EPDM) in artificial weathering environment. *Polym Degrad Stab* 92:1841–1846
9. Mavrikakis NC, Mikropoulos PN, Siderakis K (2017) Evaluation of field-ageing effects on insulating materials of composite suspension insulators. *IEEE Trans Dielectr Electr Insul* 24:490–498
10. Zhao Q, Li X, Gao J (2008) Surface degradation of ethylene–propylene–diene monomer (EPDM) containing 5-ethylidene-2-norbornene (ENB) as diene in artificial weathering environment. *Polym Degrad Stab* 93:692–699
11. Ehsani M, Borsi H, Gockenbach E, Morshedean J, Bakhshandeh GR (2004) An investigation of dynamic mechanical, thermal, and electrical properties of housing materials for outdoor polymeric insulators. *Eur Polym J* 40:2495–2503
12. Ghunem RA, Tay L-L, Terrab H, El-Hag AH (2016) Analysis of service-aged 200 kV and 400 kV silicone rubber insulation in the Gulf region. *IEEE Trans Dielectr Electr Insul* 23:3539–3546
13. Nasrat LS, Ibrahim AA, Mortadda HA (2014) Effect of environmental desert conditions on the performance of hydrophobic polymer insulators surfaces. *Int J Emerg Technol and Advanced Eng* 4:567–574
14. Khan Y (2009) Hydrophobic characteristics of EPDM composite insulators in simulated arid desert environment, vol 57. World Academy of Science, Engineering and Technology
15. Ehsani M, Bakhshandeh GR, Morshedean J, Borsi H, Gockenbach E, Shayegani AA (2007) The dielectric behavior of outdoor high-voltage polymeric insulation due to environmental aging. *Eur Trans Electr Power* 17:47–59 (2007/01/01 2006)
16. Bok-Hee Y, Chan-Su H (2005) Surface degradation of HTV silicone rubber and EPDM used for outdoor insulators under accelerated ultraviolet weathering condition. *IEEE Trans Dielectr Electr Insul* 12:1015–1024
17. Nasrat LS, Sharkawy RM (2007) An investigation into the electrical properties of rubber blends for insulators. In: 2007 electrical insulation conference and electrical manufacturing expo, 2007, pp 146–149
18. Chanliau-Blanot M, Nardiim M, Donnet J, Papirer E, Roche G, Laurensen P, Rossignol G (1989) Temperature dependence of the mechanical properties of EPDM rubber-polyethylene blends filled with aluminium hydrate particles. *J Mater Sci* 24:641–648
19. IOF Standardization, ISO 6721-11 (2012) Plastics, determination of dynamic mechanical properties: glass transition temperature: ISO, 2012
20. Sundararajan R, Mohammed A, Soundarajan E, Graves J (2003) Field and lab aging of EP compound arresters. In: 2003 annual report conference on electrical insulation and dielectric phenomena, 2003, pp 426–429
21. Xu Y, He Y, Zeng F, Zhang R (1999) Aging in EPDM used for outdoor insulation. *IEEE Trans Dielectr Electr Insul* 6:60–65
22. Saldivar-Guerrero R, Hernández-Corona R, Lopez-Gonzalez FA, Rejón-García L, Romero-Baizabal V (2014) Application of unusual techniques for characterizing ageing on polymeric electrical insulation. *Electric Power Syst Res* 117:202–209
23. Nedjar M, Boubakeur A, Beroual A, Bourmane M (2003) Thermal aging of polyvinyl chloride used in electrical insulation. *Ann de Chim Sci des Matér* 28:97–104 (2003/09/01 2003)
24. Field AP (2009) Discovering statistics using SPSS: (and sex, drugs and rock ‘n’ roll), 3rd edn. SAGE Publications, Los Angeles
25. Xu Q, Majlingova A, Zachar M, Jin C, Jiang Y (2012) Correlation analysis of cone calorimetry test data assessment of the procedure with tests of different polymers. *J Therm Anal Calor* 110:65–70 (2012/10/01 2012)
26. Puth M-T, Neuhäuser M, Ruxton GD (2015) Effective use of Spearman’s and Kendall’s correlation coefficients for association between two measured traits. *Anim Behav* 102:77–84 (2015/04/01/2015)
27. Bouguedad D, Mekhaldi A, Jbara O, Rondot S, Hadjadj A, Douglade J, Dony P (2015) Physico-chemical study of thermally aged EPDM used in power cables insulation. *IEEE Trans Dielectr Electr Insul* 22:3207–3215
28. Sichina WJ (2000) Characterization of EPDM elastomers using DSC, P. Instruments, Ed. PerkinElmer Instruments, Waltham
29. Sáenz De Juano-Arbona V, Vallés-Lluch A, Contat-Rodrigo L, Ribes-Greus A (2002) Chemical and thermal characterization of high- and low-density irradiated polyethylenes. *J Appl Polym Sci* 86:1953–1958
30. Luo P, Xu Y, Gu X, Liao Y, Cui J, Lu Z, Ren Z (2013) Thermal and mechanical properties analysis for EHV XLPE cables with different operating years. In: Electrical insulation and dielectric phenomena (CEIDP), 2013 IEEE conference on, 2013, pp 47–51
31. Boukezzi L, Boubakeur A, Laurent C, Lallouani M (2008) Observations on structural changes under thermal ageing of cross-linked polyethylene used as power cables insulation. *Iran Polym J* 17:611–624
32. Nobrega AM, Martinez MLB, de Queiroz AAA (2013) Investigation and analysis of electrical aging of XLPE insulation for medium voltage covered conductors manufactured in Brazil. *IEEE Trans Dielectr Electr Insul* 20:628–640
33. Characterization of epoxy reinforced glass by DSC and DMA. <http://www.tainstruments.com/pdf/literature/TS66.pdf>
34. Koleske JV (1995) Paint and coating testing manual: of the Gardner-Sward handbook. Paint testing manual
35. Xian G, Karbhari VM (2007) DMTA based investigation of hygrothermal ageing of an epoxy system used in rehabilitation. *J Appl Polym Sci* 104:1084–1094
36. Zhao J, Yang R, Iervolino R, Barbera S (2015) Investigation of crosslinking in the thermooxidative aging of nitrile–butadiene rubber. *J Appl Polym Sci* 132:41319-1–41319-5. <https://doi.org/10.1002/app.41319>
37. Chailan JF, Boiteux G, Chauchard J, Pinel B, Seytre G (1995) Viscoelastic and dielectric study of thermally aged ethylene–propylene diene monomer (EPDM) compounds. *Polym Degrad Stab* 47:397–403 (1995/01/01 1995)
38. McDonnell D, Balfé N, O’Donnell GE (2018) Analysis of the effects of chemical ageing of ethylene-propylene diene monomer by chemical, spectroscopic, and thermal means. *Polym Test* 65:116–124 (2018/02/01/2018)
39. Kömmling A, Jaunich M, Wolff D (2016) Revealing effects of chain scission during ageing of EPDM rubber using relaxation and recovery experiment. *Polym Test* 56:261–268
40. Seyler RJ (ed) (1994) Assignment of the glass transition. *Astm International*
41. Rahman MS, Al-Marhubi IM, Al-Mahrouqi A (2007) Measurement of glass transition temperature by mechanical (DMTA), thermal (DSC and MDSC), water diffusion and density methods: a comparison study. *Chem Phys Lett* 440:372–377 (2007/06/08/2007)
42. Ning N, Ma Q, Zhang Y, Zhang L, Wu H, Tian M (2014) Enhanced thermo-oxidative aging resistance of EPDM at high temperature by using synergistic antioxidants. *Polym Degrad Stab* 102:1–8
43. Noronha F, Angelini JMG, Góis NC, Mei LHI (2005) Performance development requirements for elastomers of electric power network insulators. *J Mater Process Technol* 162–163:102–108
44. Sundararajan R, Mohammed A, Chaipanit N, Karcher T, Liu Z (2004) In-service aging and degradation of 345 kV EPDM transmission line insulators in a coastal environment. *IEEE Trans Dielectr Electr Insul* 11:348–361
45. Khattak A, Amin M (2016) Accelerated aging investigation of high voltage EPDM/silica composite insulators. *J Polym Eng* 36:199–209

46. Barbeş L, Rădulescu C, Stih C (2014) ATR-FTIR spectrometry characterisation of polymeric materials. *Rom Rep Phys* 66:765–777
47. Yoshimura N, Kumagai S, Nishimura S (1999) Electrical and environmental aging of silicone rubber used in outdoor insulation. *IEEE Trans Dielectr Electr Insul* 6:632–650
48. Imakoma T, Suzuki Y, Fujii O, Nakajima I (1994) Degradation of silicone rubber housing by ultraviolet radiation. In: *Proceedings of 1994 4th international conference on properties and applications of dielectric materials (ICPADM)*, 1994, vol 1, pp 306–308
49. Moghadam MK, Taheri M, Gharazi S, Keramati M, Bahrami M, Riahi N (2016) A study of composite insulator aging using the tracking wheel test. *IEEE Trans Dielectr Electr Insul* 23:1805–1811
50. Mohammad A, Mohammad A, Salman A (2007) Hydrophobicity of silicone rubber used for outdoor insulation (An overview). *Rev Adv Mater Sci* 16:10–26
51. May J, Vallet G (1972) Contribution à l'étude des propriétés électriques de certains types de polymères à l'état solide. *RGE* 81:255–262
52. Boubakeur A, Mecheri Y, Boumerzou M (2000) Comportement diélectrique et mécanique du polyéthylène réticulé chimiquement soumis à un vieillissement thermique continu. In: *Annales de Chimie Science des Matériaux*, 2000, pp 457–470

Publisher's Note Springer Nature remains neutral with regard to jurisdictional claims in published maps and institutional affiliations.

Y. A. Bencherif received the degree of engineer in 2008 in Electrical Engineering and master degree in high voltage engineering in 2012 from the Ecole Nationale Polytechnique (ENP) of Algiers. He is currently PhD student with co-tutelle agreement at the ENP and the Faculté Polytechnique de Mons (FPMS), Mons, Belgium. His research areas include the outdoor insulators modeling, the aging of the polymeric materials used in the outdoor high voltage insulations and the artificial intelligence applications for the modeling of the high voltage insulators flashover.

A. Mekhaldi received the degree of engineer in 1984 in Electrical Engineering, Master degree in 1990 and Ph.D in High Voltage Engineering in 1999 from the Ecole Nationale Polytechnique (ENP) of Algiers. He

is currently Professor at ENP. His main research areas include discharge phenomena, outdoor insulators, polymeric cables insulation, lightning, artificial intelligence application in high voltage insulation diagnosis and electrical field computation.

J. Lobry received the Electrical Engineering and Nuclear Engineering Degrees from Faculté Polytechnique de Mons (Belgium) in 1987 and 1990, respectively. He also received the Ph.D. degree in electrical engineering from the same university in 1993. In 1987, he joined the Electrical Power Engineering Department of Faculté Polytechnique de Mons (University of Mons). Since 2015, he is attached to the General Physics Department of the same University. He is currently full Professor. He teaches General physics, High voltage engineering, Computational electromagnetics and of Power systems dynamics and stability. His research interests mainly include numerical methods in computational electromagnetics and high voltage engineering.

M. Olivier received the degree of civil engineer in 1991 in Chemical Engineering, Master degree in 1991 and Ph.D in Applied Science in 1996 from the Faculté Polytechnique de Mons in Belgium. She is currently Full Professor at the Faculty of Engineering of UMONS and the head of the department of Materials Science. Her main research areas include corrosion science, electrochemical processes, multifunctional coatings and electrochemical characterization of materials.

M. Poorteman was born in Ostend, Belgium, in 1959. He received his MSc degree in Physical Chemistry from the Free University of Brussels (VUB) in 1982 and his PhD degree in Material Science from the University of Valenciennes, France, in 1997. He is currently senior researcher and research coordinator at the Material Science department of the University of Mons, Belgium. His main scientific experience and interest are in the field of structural ceramics and composites, functional coatings applied on metal, hybrid materials and nanocomposites.

L. Bonnaud received the degree of chemist engineer from CPE in Lyon in France in 1996, her PhD degree from the National Institute of Applied Sciences (INSA) of Lyon in France in 1999. She is currently a senior research scientist at Materia Nova research center in Mons in Belgium working as project leader of regional projects, programs with industries and European projects (H2020...). Her main research activities involve synthesis, formulation, (nano) structuration and characterization of sustainable organic and hybrid materials.